JOURNAL OF MAPS
https://doi.org/10.1080/17445647.2021.1937729

Science

Glacial geomorphology of the central sector of the Cordilleran Ice Sheet, Northern British Columbia, Canada

Helen E. Dulfer and Martin Margold

Department of Physical Geography and Geoecology, Faculty of Science, Charles University, Prague, Czech Republic

ABSTRACT

Northern British Columbia was repeatedly covered by the Cordilleran Ice Sheet (CIS) during the glacial periods. However, its mountainous terrain and remote location have thus far impeded our understanding of the central sector of the ice sheet. The improved resolution of remotely sensed data provides new opportunities to unravel the glacial history of this inaccessible location. Here, we present a comprehensive map of glacial landforms for the central sector of the CIS (55° to 60° N). Seven landform categories were mapped: ice flow parallel lineations, moraines (CIS outlet glacier moraines, Late Glacial moraines and moraines of unknown origin), meltwater channels (lateral and submarginal, subglacial, proglacial, and meltwater channels of unknown origin), kame terraces, eskers (single ridges and esker complexes), perched deltas and subglacial ribs. Collectively, these landforms provide a record of the extent, thickness and behaviour of the CIS, the direction of its movement and pattern of ice retreat.

ARTICLE HISTORY
Received 27 January 2021
Revised 24 May 2021
Accepted 24 May 2021

KEYWORDS
Cordilleran Ice Sheet; glacial landforms; remote sensing

1. Introduction

Mountainous British Columbia in western Canada has been repeatedly covered by the Cordilleran Ice Sheet (CIS) during the Quaternary. At the Last Glacial Maximum (LGM), it attained a volume and area similar to that of the present-day Greenland Ice Sheet. While it has long been recognized that the high mountains in northern British Columbia played an important role in establishing the ice sheet (Clague & Ward, 2011; Davis & Mathews, 1944; Fulton, 1991), the mountainous topography and remote location have thus far impeded our understanding of the central sector of the CIS and we still do not fully comprehend its LGM configuration or pattern of ice retreat. This makes it one of the least understood areas of any ephemeral Pleistocene ice sheet.

Ice flow is well documented in British Columbia. Both Kleman et al. (2010) and Shaw et al. (2010) give generalized ice flow maps of the entire North American Ice Sheet Complex (NAISC), which was made up of the Cordilleran, Laurentide and Innuitian ice sheets at the LGM, and Arnold et al. (2016) provide a compilation of all published streamlined landforms within British Columbia. However, the Glacial Map of Canada produced by Prest et al. (1968) at a 1:5,000,000 scale is the only ice-sheet-wide map of glacial landforms for the NAISC to date. This map is sufficient for deciphering the overall ice retreat pattern of the Laurentide Ice Sheet using the occurrence of eskers, which are thought to be deposited perpendicular to the retreating ice margin, drumlin orientation and ice marginal positions delineated by moraine systems (Dyke, 2004; Dyke et al., 2003; Dyke & Prest, 1987; Margold et al., 2018). However, in northern British Columbia the majority of ice marginal positions are recorded by meltwater landforms, such as lateral meltwater channels, kame terraces, eskers and perched deltas (Lakeman et al., 2008; Margold et al., 2013a, 2013b), which are not adequately recorded on the Glacial Map of Canada. Therefore, more detailed landform mapping is required to understand retreat of the central sector of the CIS.

The increased resolution and coverage of digital elevation models (DEMs) and satellite imagery presents new opportunities to study the subglacial bed of paleo-ice sheets in detail (Chandler et al., 2018; Stokes et al., 2015). In order to gain a better understanding of the CIS, we use high resolution remotely sensed data to create a detailed glacial landform map centered on the LGM ice divide region in northern British Columbia. This map covers an area of ~200,000 km^2 located between 55–60° N and 122.6–135.5° W (Figure 1).

CONTACT Helen E. Dulfer dulferh@natur.cuni.cz Department of Physical Geography and Geoecology, Faculty of Science, Charles University, Albertov 6, 12800 Praha, Czech Republic

Supplemental data for this article can be accessed here https://doi.org/10.1080/17445647.2021.1937729

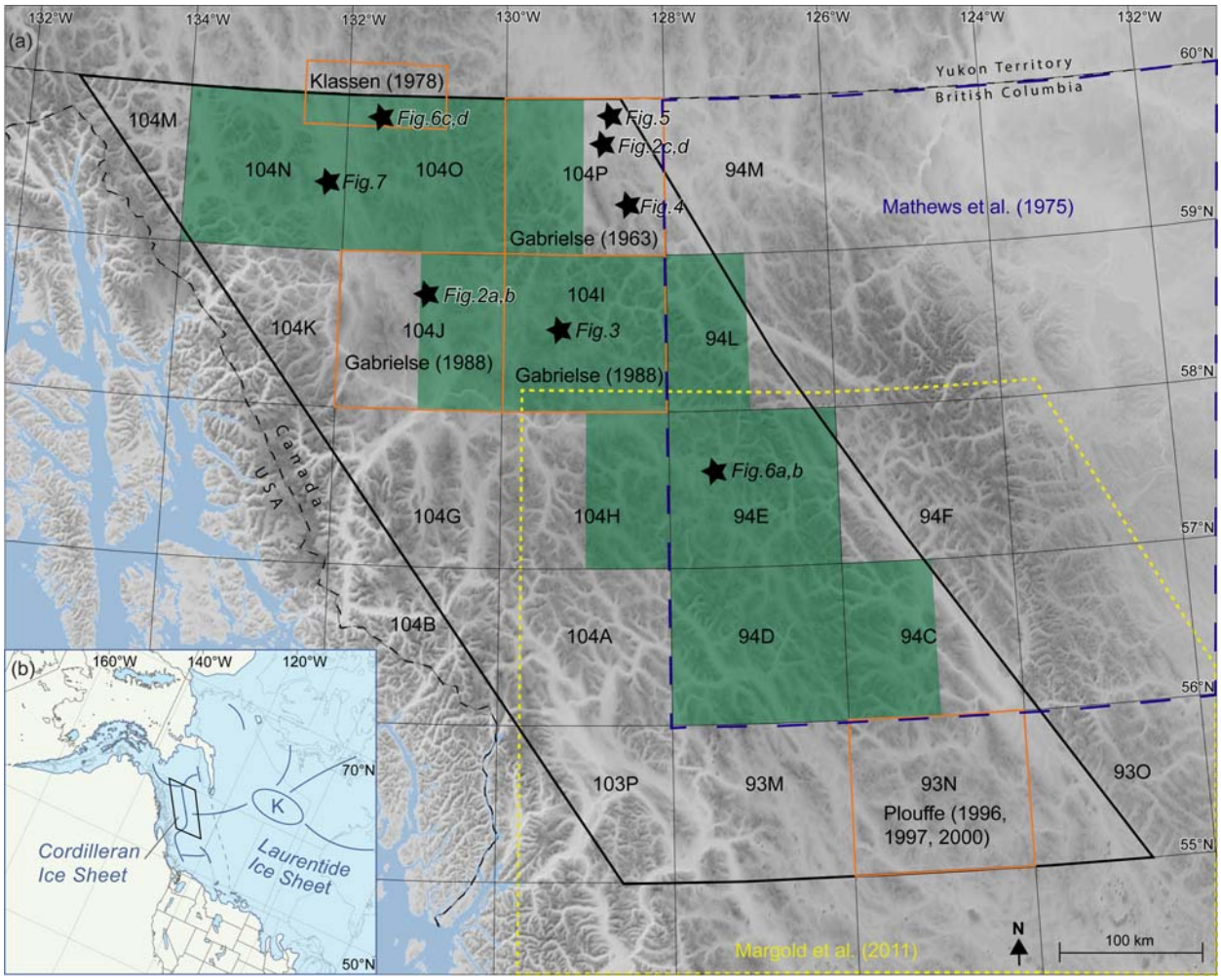

Figure 1. (a) Map showing the extent of the glacial geomorphological map produced in this study (black outline). The National Topographic System tiles that intersect with the mapped area are labelled. The green colour shows the coverage of TanDEM X DEM tiles used in this study. The orange boxes show the coverage of surficial geology maps from the Geological Survey of Canada that contain glacial landforms. The yellow box corresponds to the broad-scale glacial geomorphology map of Margold et al. (2011) and the blue box corresponds to the map area of Mathews et al. (1975). The location of the remaining figures is shown by the black stars. (b) Inset map showing the extent of the western margin of the North American Ice Sheet Complex at 22.1 cal ka BP drawn from Dalton et al. (2020) with the approximate position of the ice divides and the Keewatin ice dome (K) drawn in dark blue and the suture zone between the CIS and Laurentide ice sheet shown by the blue dashed line (Menounos et al., 2017; Margold et al., 2018). The location of the study area is shown by the black box within the Cordilleran Ice Sheet.

2. Methods

2.1. Data

Glacial geomorphological mapping was primarily undertaken in ArcMap 10.6.1 using hillshade imagery derived from the Canadian Digital Elevation Model (DEM) of 0.75 arc second spatial resolution (12–20 m; complete coverage) (Government of Canada, 2019), and high resolution satellite images from Planet Lab (3–5 m resolution) (Planet Team, 2017) and Google Earth. Additionally, the German Aerospace Centre allowed us to download TanDEM-X DEM tiles of 0.4 arc second resolution (12 m) data covering 100,000 km^2 through their science project (see Figure 1 for coverage) (German Aerospace Center, 2018).

Other data sources that were used in the identification of landforms include surficial geological maps (Gabrielse, 1963, 1988; Klassen, 1978; Margold et al., 2011; Mathews et al., 1975; Plouffe, 1996, 1997, 2000) (see Figure 1 for location of maps), generalized maps of ice flow (Kleman et al., 2010; Shaw et al., 2010), a compilation of published streamlined landforms in British Columbia (Arnold et al., 2016) and regional to local scale glacial geomorphology studies (e.g. Lakeman et al., 2008; Margold et al., 2013a, 2013b, 2014; Ryder & Maynard, 1991; Stumpf et al., 2000).

2.2. Landform mapping

The map is bound by the Yukon Territory-British Columbia border at 60° N, the Rocky Mountain Trench to the east and the Coast Mountains to the west, and the 55° N parallel to the south (Figure 1). The physiographic regions labelled on the Main Map are from Mathews (1986). A repeat-pass method was used to identify each landform through the entire

study area. To increase consistency, mapping was conducted at a variety of scales between 1:30,000 and 1:70,000 depending on landform type. Each landform has been identified from the imagery based on its morphology, spatial arrangement and association with other landforms (Table 1).

2.2.1. Ice flow parallel lineations

Ice flow parallel lineations include drumlins, flutes, grooved bedrock, and crag-and-tails. These landforms represent a variety of depositional and erosional ridges that are elongated in the direction of ice flow (e.g. Boulton & Clark, 1990a, 1990b; Clark, 1999; King et al., 2009). Ice flow parallel lineations often occur in fields or swams that are made up of hundreds of individual lineations that have regular morphology, spacing and orientation (Figure 2). Where the stoss and lee side of a lineation was identified, for example, by the tapering sedimentary tail on the lee side of the crag-and-tails, the ice flow direction has been drawn on the Main Map. Complex arrangements of lineations with different orientations reflect different ice flow phases, which can be used to determine how flow changed over time (e.g. Greenwood & Clark, 2009; Jansson et al., 2002; Kleman et al., 1997).

2.2.2. Meltwater channels

Meltwater channels are formed in three main positions within an ice sheet: they are formed by water flowing along the ice margins (lateral and submarginal; Figure 3), by channelized flow at the bed of the ice sheet (subglacial; Figure 4), and by meltwater draining away from the ice sheet terminus (proglacial) (Greenwood et al., 2007, 2016; Mannerfelt, 1949; Margold et al., 2011). Each of these types of meltwater channels provide important paleo-glaciological information about the former ice sheet and therefore, where possible, they were distinguished based on their morphology and relationship to the surrounding topography (Table 1). However, sometimes a channel may transport different sources of meltwater at different stages of the ice sheet's evolution and a channel may have been draining water from both a glacially dominated source and from a fluvial or glaciofluvial source at a later stage. Therefore, where the meltwater channels has a glacial source but the type of meltwater channel could not be identified, they have been mapped as meltwater channels of unknown origin.

2.2.3. Kame terraces

Kame terraces are narrow, gently sloping accumulations of glaciofluvial sediment perched on valley sides that are formed by deposition of sediment along the lateral margins of a valley glacier or an ice sheet lobe (Borsellino et al., 2017; Evans, 2005; Turner et al., 2014) (Figure 3). They often occur in a series and are distinguished from river terraces by their high elevation valley margin location and close association with other glaciofluvial landforms, such as lateral and submarginal meltwater channels.

2.2.4. Eskers

Eskers are linear depositional ridges composed of glaciofluvial sand and gravel that are deposited by meltwater flowing through conduits beneath ice masses (Hebrand & Åmark, 1989; Shreve, 1985; Storrar et al., 2014). They exist as individual segments that often align to form networks up to 200 km in length and their morphology can vary from continuous single ridges to multiple ridged eskers to large esker complexes or deltas (Margold et al., 2011; Storrar et al., 2020). Within esker complexes it can be difficult to distinguish the individual esker ridges and where this occurs they are mapped as a polygon (Figure 5). It is hypothesized that eskers form within Röthlisberger channels (R-channels) that are aligned roughly normal to the ice margin, and, therefore, they record the meltwater drainage pattern and ice marginal positions during ice retreat (Brennand, 2000; Hewitt & Creyts, 2019; Livingstone et al., 2015; Stroeven et al., 2016).

2.2.5. Moraines

Moraines occur as sharp-crested, straight or arcuate-shaped ridges that are formed by the deposition or deformation of glacigenic sediment at the margins of active glaciers (Benn & Evans, 2010). A number of previous studies have recognized that moraines of different origins are located within northern British Columbia (Lakeman et al., 2008; Menounos et al., 2017; Ryder & Maynard, 1991). In particular, Lakeman et al. (2008) describe large, regionally extensive, sharp-crested moraines that extend up to 9 km beyond Little Ice Age moraines, which are interpreted to be deposited by a late Pleistocene advance of independent alpine glaciers (Lakeman et al., 2008; Menounos et al., 2017). While morphologically similar moraines have been noted across the Cassiar and Omineca mountains, their distribution has never been mapped.

We have mapped three different types of moraines based on their morphology, orientation and location: (1) CIS outlet glacier moraines; (2) Late Glacial moraines; and (3) moraines of unknown origin. The first type of moraine was deposited by outlet glaciers of the CIS that were flowing along glacial troughs during deglaciation (Figure 6(c, d)) and they are identified by their close association with other ice marginal landforms, such as kame terraces and lateral and submarginal meltwater channels. The second type of moraine was deposited by glaciers emanating from mountain peaks, and they are identified as sharp-crested ridges that form on cirque and valley floors (Figure 6(a, b)). The final category is used when the origin of the

Table 1. Diagnostic criteria for the identification of glacial geomorphological landforms from remotely sensed data (after Greenwood et al., 2007; Margold & Jansson, 2012; Norris et al., 2017).

Landform		Diagnostics used for landform identification	Mapping Symbol
Ice flow parallel lineations		Elongate landforms with contrasting tone (brightness and colour) on either side of the linear crestline. Possible identification errors include confusion with non-glacial bedrock structures and straight moraines. The lineations are differentiated from straight moraines by their smaller size and proximity to other lineations of similar orientations.	Landform crest is drawn as a single line
Meltwater channels	Lateral and submarginal	Incised topography with the edges of channels defined by contrasting tone. Often perched on valley sides. Regularly form a series of channels that are parallel to each other and dip in the same direction. Low to medium sinuosity. Length varies between 100 m and 15 km. The maximum channel width is 500 m. Channel networks uncommon. Submarginal meltwater channels may terminate in downslope chutes.	Centre of incised topography drawn as a single line
	Subglacial	Incised topography with the edges of channels defined by contrasting tone. Undulating long profile whereby flow can be oblique to the slope. Often associated with eskers. Potholes common. Medium to high sinuosity. Bifurcating and anastomosing channels. Length varies between 500 m to 20 km and they are <500 m wide.	
	Proglacial	Incised topography with the edges of channels defined by contrasting tone. Flow is directly downslope. Large width (up to 1 km) and between 1 km to 15 km in length. High sinuosity. Can cross-cut subglacial landforms such as eskers.	
	Unknown origin	Incised topography with the edges of channels defined by contrasting tone. The channel has a glacial origin but the position of the channel within the ice sheet could not be identified.	
Kame terraces		Elongate, flat-topped, semi-continuous landforms that have contrasting tone along the edges. They are often perched on valley sides. Usually <100 m wide.	A single line drawn along the break in slope
Eskers	Ridges	Sharp, sinuous ridges (100–300 m wide) that exhibit variation in tone across their crestline. Often form on the valley floor. High sinuosity. Can occur oblique to the slope. Semi-continuous ridges may be traced for tens to hundreds of kms.	Landform crest drawn as a single line
	Complexes	Occur when esker ridges form complex branching networks. Difficult to distinguish and trace individual ridges. Can be associated with deltas.	Landform outline drawn as a polygon
Moraines	CIS outlet glacier moraines	Broadly linear ridges that exhibit variation in tone across their crestline and shadowing due to changes in the relative relief. Exhibit both sharp and broad ridge crests. Associated with other ice contact landforms, such as deltas, kame terraces and meltwater channels. Lateral moraines perched on valley sides occur roughly parallel with the contours.	Landform crest drawn as a single line
	Late Glacial moraines	Broadly linear ridges exhibit variation in tone across their crestline and shadowing due to changes in the relative relief. Terminal moraines are located at the end of a valley or cirque and have an arcuate shape. Often exhibit sharp ridge crests and may occur as multiple ridges.	
	Unknown origin	Broadly linear ridges which exhibit variation in tone across their crestline and shadowing due to changes in the relative relief. The origin of the moraine could not be identified. Distinguished from eskers based on their lack of sinuosity and location within a valley.	
Perched deltas		Flat-topped accumulations of glaciofluvial sediment with steeply dipping frontal beds.	Landform outline drawn as a polygon
Subglacial ribs		Ridges of sediment lying transverse to the flow direction. Typically occur in groups or swarms. May be drumlanised. Ridge sizes are highly variable.	Landform outline mapped as a polygon around the break in slope.

moraine is uncertain and also includes moraines that could have been formed during the ice advance phase.

2.2.6. Perched deltas

Deltas are deposited when sediment that is transported by a river or stream is discharged into a standing body of water (e.g. a lake) and they typically have a flat top and steeply dipping front. As an ice margin retreats it can block the natural water drainage pathways resulting in transient ice-dammed lakes. Sediments deposited into these glacial lakes form deltas that remain perched on valley slopes once the glacial lake drains (Mannerfelt, 1949; Stroeven et al., 2016) (Figure 3). It is possible that river terraces could be mistaken for perched deltas because they have a similar morphology. In order to reduce misidentification, we have only mapped deltas that are perched above the present-day rivers.

2.2.7. Subglacial ribs

Subglacial ribs are large, regularly spaced transverse ridges that are formed subglacially (Aylsworth & Shilts, 1989; Dunlop & Clark, 2006; Hättestrand & Kleman, 1999; Lundqvist, 1989) (Figure 7). While these landforms have a variety of names within the literature, including Rogen or ribbed moraines, here we use the non-genetic term subglacial ribs following the BRITICE Glacial Map (Clark et al., 2018). Although the morphology and size of subglacial ribs is highly variable (Dunlop & Clark, 2006; Stokes et al., 2016), they often have a curved or anastomosing pattern. Individual ridges usually have an asymmetric profile and multiple ribs often occur together forming fields.

2.3. Accuracy and comprehensiveness

We believe the distribution in landforms presented on this map reflects the true distribution pattern rather than being related to variable data sources. Although TanDEM-X tiles only cover half of our mapped area, we found that this higher resolution data did not allow us to identify and map new landforms, it rather allowed us to map certain landforms, such as moraines, with more confidence. However, some moraines, eskers and lateral and submarginal meltwater channels are near the resolution limit of the remotely sensed data, and therefore, it is possible that smaller features may have been missed. Landforms that may be misinterpreted, such as eskers and moraines, are listed in Table 1.

3. Results

3.1. Ice flow parallel lineations

In total 52,300 ice flow parallel lineations were mapped during this study. Overall, our lineations are consistent with the generalized ice flow maps of Kleman et al. (2010) and Shaw et al. (2010) and the detailed ice flow indicator compilation by Arnold et al. (2016). The ice flow parallel lineations range in size from tens of meters to 2 km in length but mega-scale glacial lineations were not identified within the mapped area.

Swarms of ice flow parallel lineations occur throughout the mapped area. Their location within the mountainous terrain, either at the bottom of large valleys (e.g. Teslin Trench), on high elevation peaks and plateaus, and on the plains surrounding the mountainous region, e.g. the Liard Lowland (Figure 2(c, d)), likely corresponds to different phases of ice flow. Furthermore, it is common for the orientation of the ice flow parallel lineations at high elevations (e.g. on mountain summits) to differ from the orientation of those located in the adjacent valleys (e.g. Atlin; see Main Map).

On the floor of some valleys ice flow parallel lineations overprint subglacial ribs (e.g. Teslin Trench). At other locations, they form a divergent, fan-shaped pattern (e.g. Liard Lowland; Figure 2(c, d)). Occasionally, the lineations have complex orientations with cross-cutting relationships, implying there were significant differences in the ice flow direction at different stages of ice sheet evolution (Figure 2(a, b)).

3.2. Meltwater channels

3.2.1. Lateral and submarginal meltwater channels

In total 18,420 lateral and submarginal meltwater channels were mapped during this study, making them the most common type of meltwater channel in northern British Columbia. These meltwater channels vary in length from a few hundred meters to 15 km and they generally have a low sinuosity, with sinuosity increasing when the channel becomes submarginal. Lateral and submarginal meltwater channels can occur at any elevation: the highest meltwater channels often cut small notches in ridges or spurs emanating from mountain peaks (up to 1750m asl); and the lowest channels form close to the valley floor (down to 700 m asl).

These channels are the most distinctive glacial landform identified within the Cassiar and Omineca Mountains, where thousands of channels have been mapped, while they are noticeably absent from the Coast and Skeena mountains. Additionally, while the studies of Margold et al. (2011, 2013a, 2013b) determine the overall direction of glacial meltwater flow through generalized mapping of lateral meltwater channels, this study presents the first map of individual meltwater channels for the central sector of the CIS.

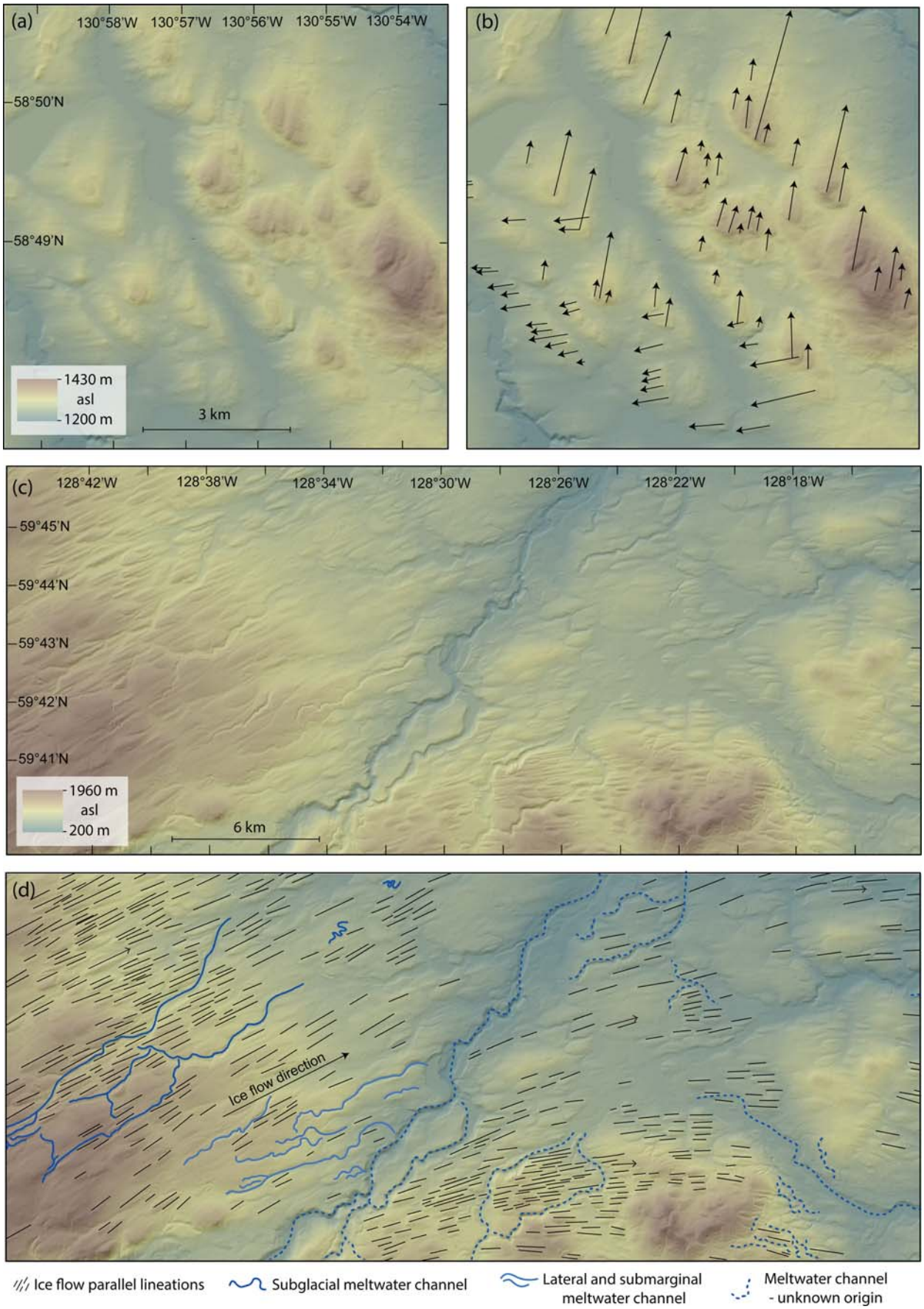

Figure 2. Examples of ice flow parallel lineations (a) Tandem X-derived hillshade imagery and (b) geomorphological mapping of north–south oriented lineations overprinted by east–west oriented lineations on the Tanzilla Plateau. (c) Canadian DEM-derived hillshade imagery and (d) geomorphological mapping on the plains of the Liard Lowland. These ice flow parallel lineations form a divergent pattern. The location of these figures is shown in Figure 1.

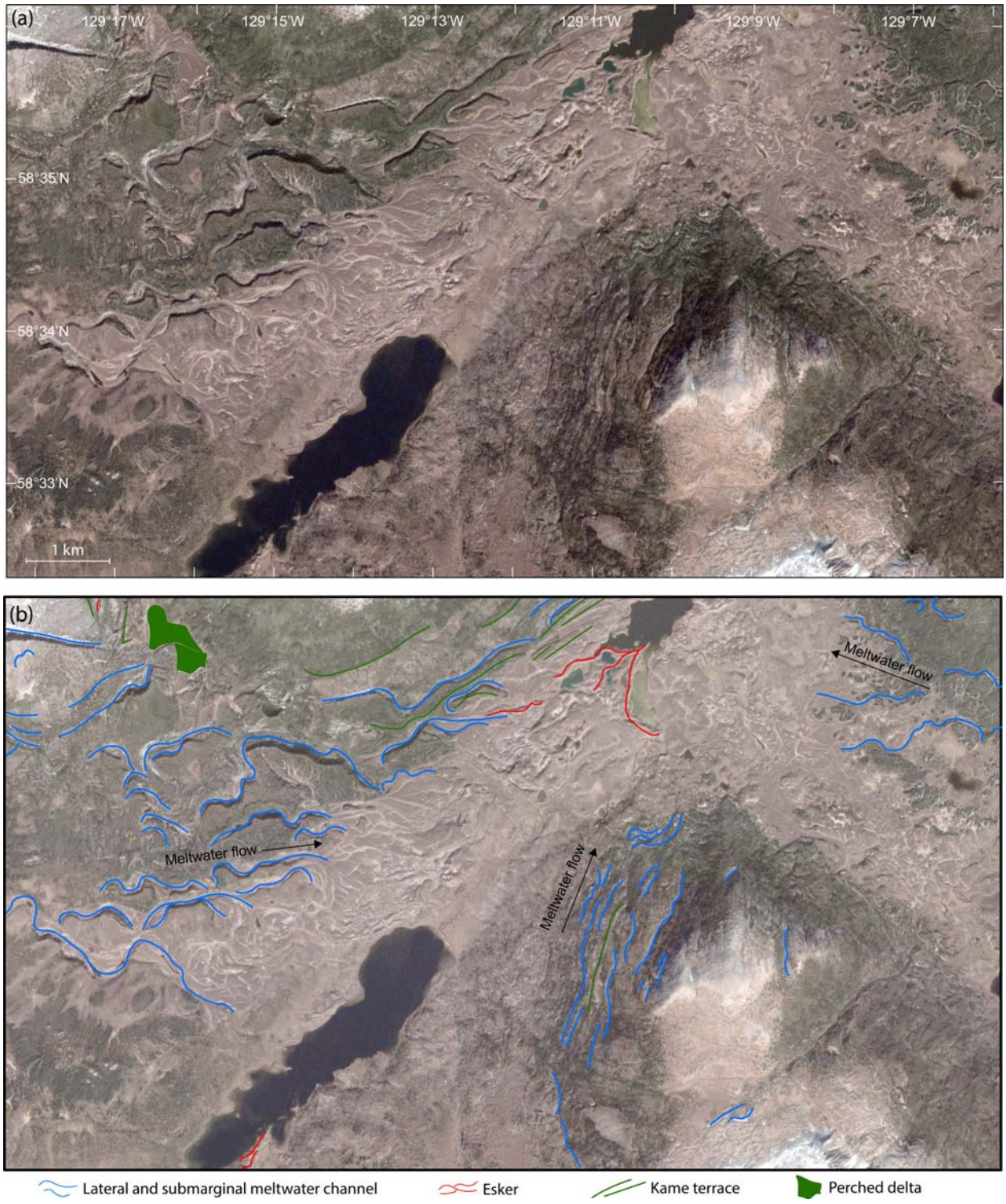

Figure 3. (a) High-resolution Planet Lab satellite imagery and (b) geomorphological mapping. Lateral and submarginal meltwater channels and kame terraces are perched on the valley sides. Both landforms occur subparallel with the topography and the direction of meltwater flow is towards the northeast. Flat-topped perched deltas can also be seen in the satellite imagery and esker ridges occur on the valley bottom. The location of this figure is shown in Figure 1.

3.2.2. Subglacial meltwater channels

In total 245 subglacial meltwater channels were mapped during this study. While they can occur at any topographic position, and sometimes dissect mountain ridges, they are most common on the valley floor. The mapped subglacial channels often contain plunge pools that form present-day ponds within the channel (Figure 4). The majority of large subglacial meltwater channels (widths between 200 and 800 m) are located in the Liard Lowlands (see Main Map). Here some of the subglacial meltwater channels are aligned with eskers and esker complexes and have roughly consistent orientations over tens of km.

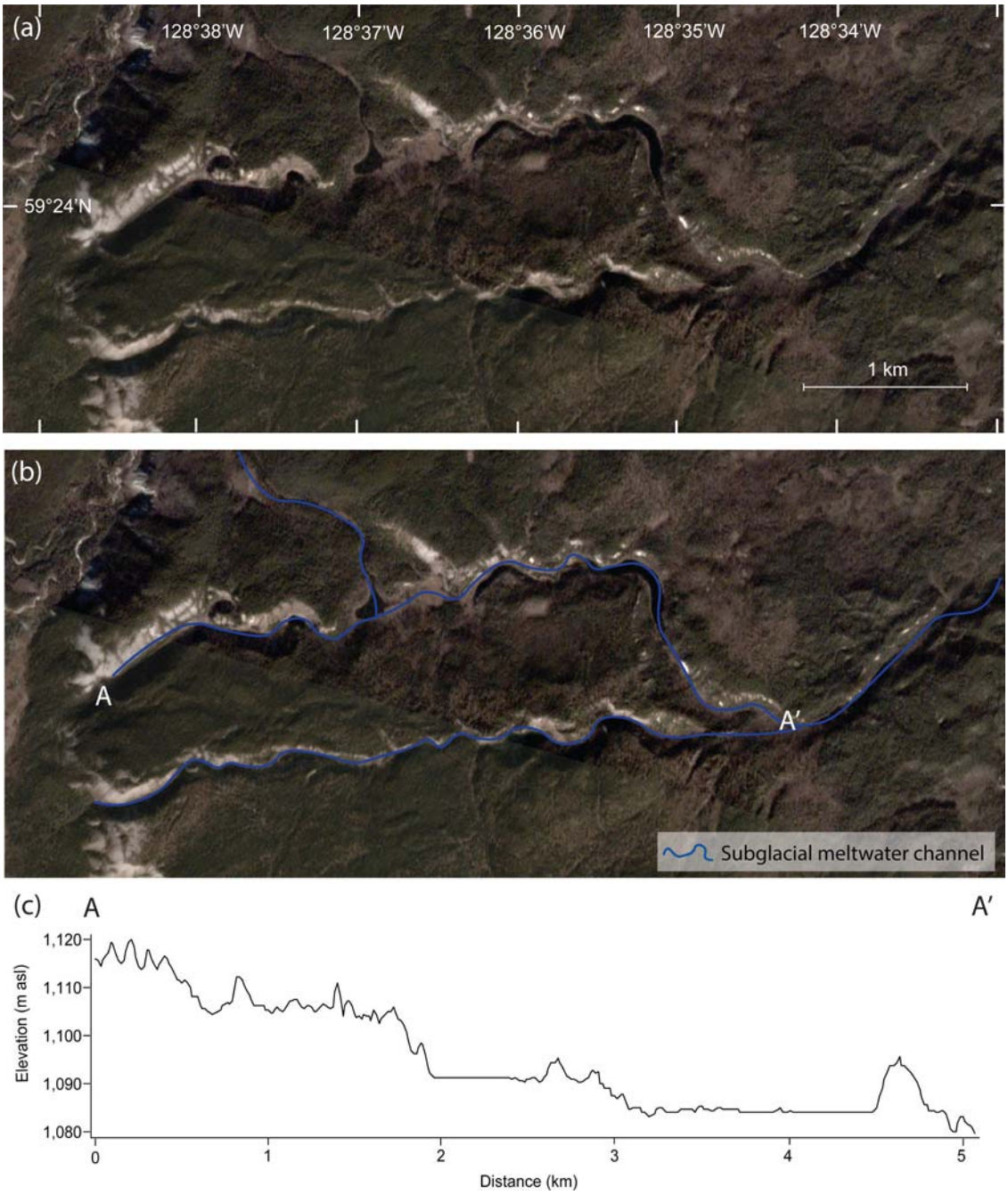

Figure 4. Example of subglacial meltwater channels (a) high-resolution Planet Lab satellite imagery, (b) geomorphological mapping and (c) elevation profile along the channel A–A′ produced using the Canadian DEM. The elevation profile shows the channel has an undulating long profile, which is a unique feature of subglacial meltwater channels (Table 1), and plunge pools can be seen in the satellite imagery. The location of these figures is shown in Figure 1.

3.2.3. Proglacial meltwater channels

In total 9 wide, meandering proglacial meltwater channels (up to 1 km wide) were identified within the map area. These meltwater channels are primarily recognized based on their relationship to other glacial landforms. For example, the large proglacial meltwater channels in the Liard Lowland crosscut esker complexes and subglacial meltwater channels (see Main Map), indicating that large volumes of water flowed through these channels after the ice margin retreated.

3.2.4. Meltwater channels of unknown origin

In total 304 glacial meltwater channels were identified within the map area where the source of glacial meltwater could not be identified. They vary in length from a few hundred meters to 30 km.

3.3. Kame terraces

In total 983 kame terraces were mapped in the study area and they are located on the valley walls throughout the Omineca and Cassiar mountains. They vary in

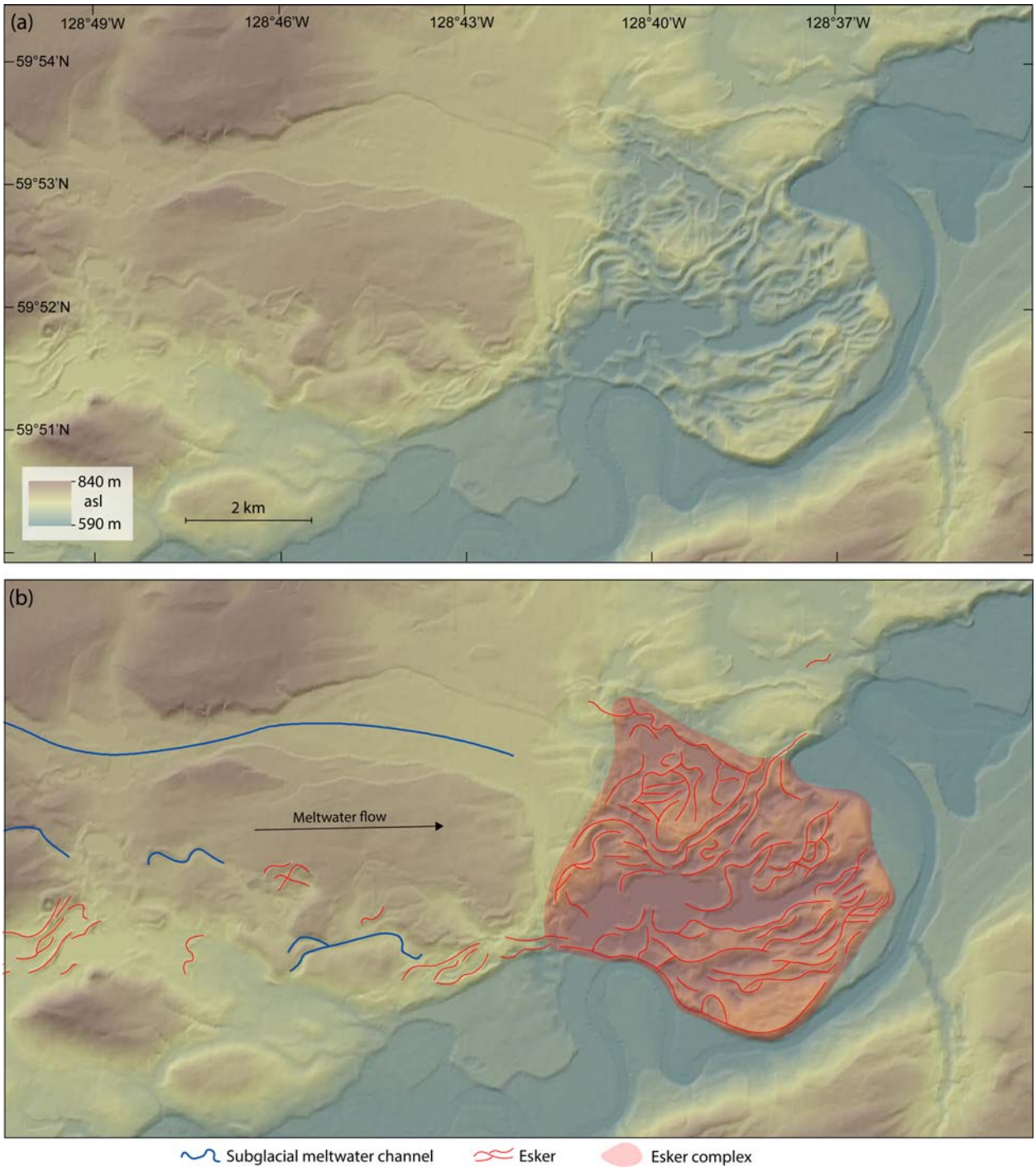

Figure 5. Example of an esker complex. (a) Canadian DEM-derived hillshade imagery and (b) geomorphological mapping of esker ridges, an esker complex and subglacial meltwater channels. This esker complex is located in the Liard Lowland (see Figure 1 for location).

size from a few hundred meters to 1 km in length and they are up to a few hundred meters wide. They are often associated with other ice marginal landforms, such as lateral and submarginal meltwater channels.

3.4. Eskers

3.4.1. Esker ridges

Esker ridges have been mapped throughout the study area with the exception of the Coast Mountains, Nass Depression and western Skeena Mountains. In total 3574 esker ridges were mapped and they are most commonly located on valley floors, where semi-continuous ridges can be traced for tens of km and anastomosing ridges are common. At some locations esker ridges have a preferred orientation. For example, the esker ridges located in the Cassiar Mountains and the Liard Lowland in the northeast corner of the map are generally oriented in a northeast–southwest direction.

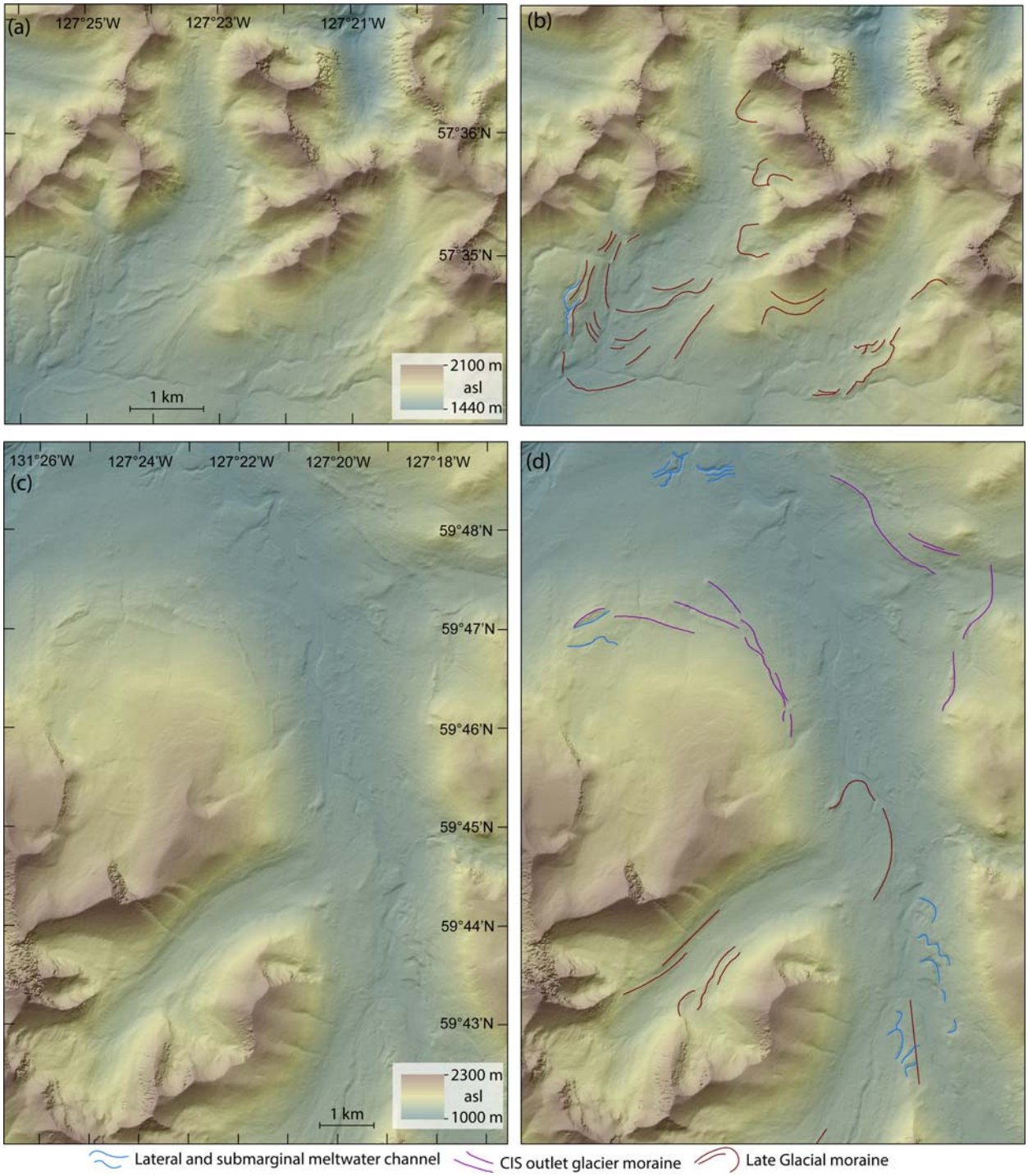

Figure 6. Examples of CIS outlet glacier moraines and Late Glacial moraines. (a) Tandem X-derived hillshade imagery and (b) geomorphological mapping of arcuate-shaped, sharp-crested, multi-ridged, Late Glacial moraines. (c) Tandem X-derived hillshade imagery and (d) geomorphological mapping of Late Glacial moraines formed by local mountain glaciers and CIS outlet glacier moraines formed along the valley wall. The location of these figures is shown in Figure 1.

3.4.2. Esker complexes

In total 80 esker complexes were mapped in this study, which range from 1 to 15 km in length. Esker complexes are primarily located on the eastern side of the mapped area, with the largest complexes occurring within the Liard Lowland and the Rocky Mountain Trench (see Main Map). However, they also occur on the floor of some valleys within the Cassiar and Omineca mountains.

3.5. Moraines

3.5.1. CIS outlet glacier moraines

In total 97 ridges have been mapped as CIS outlet glacier moraines during this study. These moraines are made up of both single and multiple ridges and they vary in length between 2 and 4 km, with widths of ~250 m. All of CIS outlet glacier moraines are located within the Cassiar Mountains, with the exception of 5

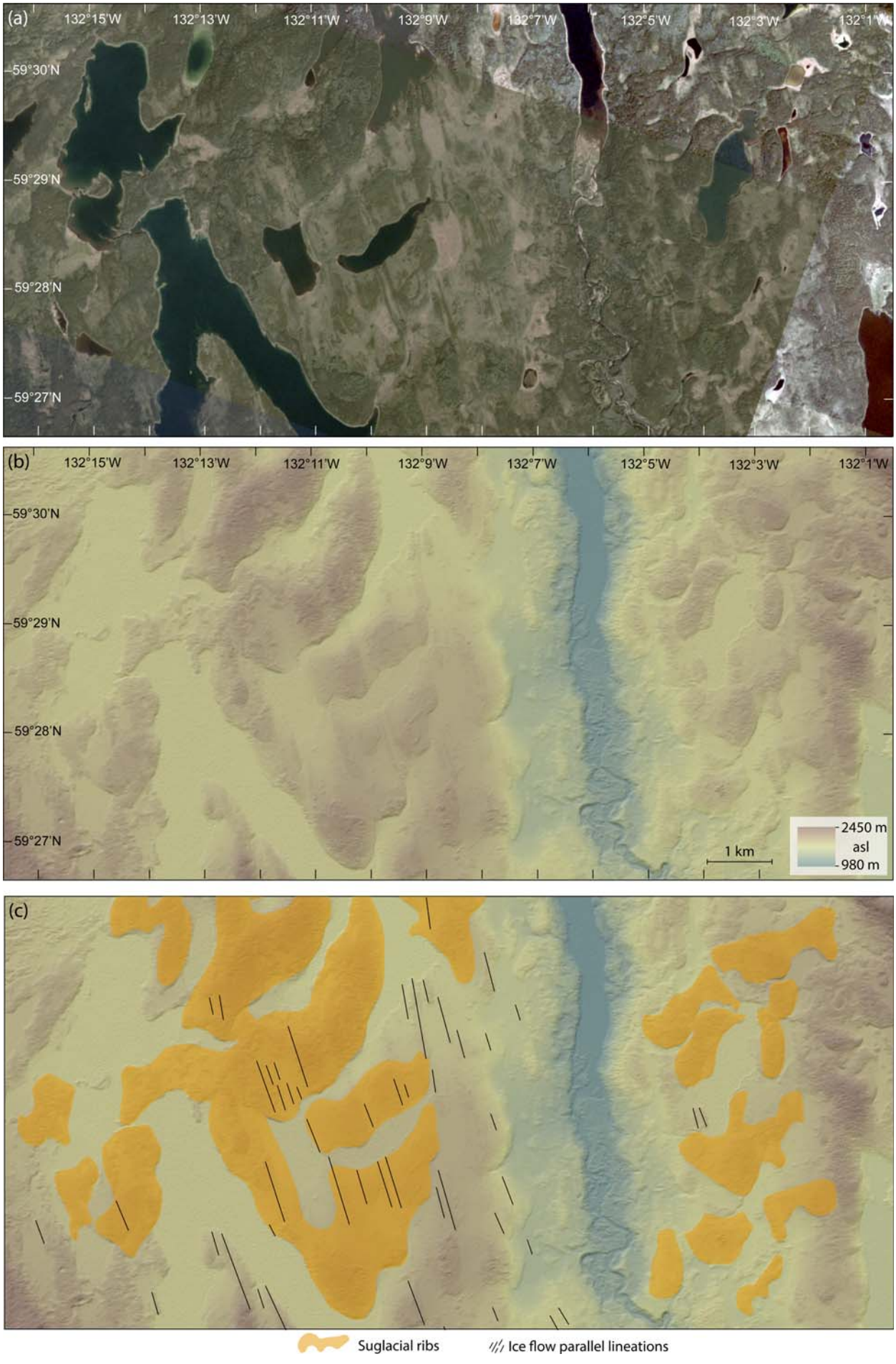

Figure 7. (a) High-resolution Planet Lab satellite imagery, (b) Tandem X-derived hillshade imagery and (c) geomorphological mapping of subglacial ribs and ice flow parallel lineations. The location of this figure is shown in Figure 1.

moraine ridges that were mapped in the Omineca Mountains.

3.5.2. Late Glacial moraines

In total 1459 ridges have been mapped as Late Glacial moraines, making them the most common type of moraine mapped within the study area. These moraines are made up of single and multiple ridges and they vary in length from a few hundred meters up to a few kilometers. The largest Late Glacial moraine, which is located southeast of Tuya Lake (see Main Map), consists of multiple ridges with a total length of 8 km. The minimum elevation of the Late Glacial moraines is 1100 m asl. They are primarily located in the Cassiar and Omineca mountains, but, they also occur on the Tuku Plateau and Meszah Peak, while they are absent from the Skeena and Coast mountains.

3.5.3. Moraines of unknown origin

In total 378 ridges have been mapped as moraines of unknown origin (20%). Some of these ridges have a subdued topography and may have been formed during the ice sheet advance stage, however, this cannot be determined by remote sensing methods alone.

3.6. Perched deltas

In total 223 perched deltas were mapped during this study, which range in size from a few hundred meters to 16 km wide and 20 km long. The largest perched deltas are located in the Liard Lowland and along the Rocky Mountain Trench, while smaller perched deltas are concentrated in the Cassiar and Omineca mountains.

3.7. Subglacial ribs

Here we map subglacial ribs in northern British Columbia for the first time with a total of 683 ribs mapped. These subglacial ribs have a variety of sizes and shapes, with the largest ribs being 5 km long and 1 km wide. The ribs are spaced between 500 m and 1 km apart. While subglacial ribs occur on valley floors in a few locations across the mapped area, the majority are located within the Teslin Trench. Ice flow parallel lineations are sometimes superimposed on the subglacial ribs.

4. Regional implications and conclusions

The Main Map provides a detailed broad-scale glacial landform record of the central sector of the CIS. Overall, the mapped landforms are consistent with the landform record described in the existing literature (e.g. Kleman et al., 2010; Lakeman et al., 2008; Margold et al., 2013a, 2013b, 2014; Shaw et al., 2010). For example, our mapped ice flow parallel lineations generally agree with the generalized flow maps of Kleman et al. (2010) and Shaw et al. (2010) and the ice flow indicator map of Arnold et al. (2016). However, our glacial landform map presents the first large-scale, detailed map for many of the landforms (e.g. lateral and submarginal meltwater channels and Late Glacial moraines), and therefore, thousands of previously unrecognized glacial landforms, including eskers, moraines, meltwater channels, kame terraces and subglacial ribs, have been identified and mapped using the high resolution remotely sensed data. The majority of newly mapped landforms are located in the Cassiar and Omineca mountains.

It is clear from the map that there is a marked difference between the glacial landform assemblage within the Cassiar and Omineca mountains to the east, where thousands of lateral meltwater channels, eskers and Late Glacial moraines have been mapped, and the Skeena and Coast mountains to the west, where these glacial landforms are noticeably absent. This glacial geomorphological map can now be used to unravel the complex glacial history beneath the LGM ice divide region of the CIS and help us to better understand the advance and retreat dynamics of this ephemeral Pleistocene ice sheet.

Software

The hillshade surfaces were produced from the DEM data within ESRI ArcMap 10.6.1. On-screen digitizing of landform crestlines and break-in-slopes was conducted in ArcMap 10.6.1 in the ESRI shapefile format and in Google Earth as KML files that were then converted to ESRI shapefiles in ArcMap 10.6.1. The pdf map was exported and the final map was created in Adobe Illustrator 2020.

Availability of data

The ESRI shapefiles produced for each glacial landform type are supplied with this paper.

Acknowledgements

The authors would like to thank Planet Lab who made the high resolution satellite imagery used in this study (4-band PlanetScope scenes) available to us through their education and research program and the German Aerospace Centre for awarding us a TandDEM-X Science DEM project, which allowed us to download the high resolution TanDEM X DEM (0.4 arc second resolution) covering approximately half of the mapped area (100,000 km^2). The authors thank Stephen Livingstone, Makram Murad-al-shaikh, Arjen Stroeven and Jasper Knight for their constructive reviews of the map and manuscript.

Disclosure statement

No potential conflict of interest was reported by the author(s).

Funding

This research was supported by the Charles University Grant Agency (GAUK 432119).

References

Arnold, H., Ferbey, T., & Hickin, A. S. (2016). *Ice-flow indicator complation, British Columbia and Yukon*. Geological Survey of Canada, Open File 8083. https://doi.org/10.4095/298865

Aylsworth, J. M., & Shilts, W. W. (1989). Bedforms of the Keewatin Ice sheet, Canada. *Sedimentary Geology*, *62*(2-4), 407–428. https://doi.org/10.1016/0037-0738(89)90129-2

Benn, D., & Evans, D. (2010). *Glaciers and glaciation (2nd ed.)*. Hodder.

Borsellino, R., Shulmeister, J., & Winkler, S. (2017). Glacial geomorphology of the brabazon & butler downs, rangitata valley, south island, New Zealand. *Journal of Maps*, *13*(2), 502–510. https://doi.org/10.1080/17445647.2017.1336122

Boulton, G. S., & Clark, C. D. (1990a). A highly mobile Laurentide Ice Sheet revealed by satellite images of glacial lineations. *Nature*, *346*(6287), 813–817. https://doi.org/10.1038/346813a0

Boulton, G. S., & Clark, C. D. (1990b). The Laurentide ice sheet through the last glacial cycle: The topology of drift lineations as a key to the dynamic behaviour of former ice sheets. *Transactions of the Royal Society of Edinburgh: Earth Sciences*, *81*(4), 327–347. https://doi.org/10.1017/S0263593300020836

Brennand, T. A. (2000). Deglacial meltwater drainage and glaciodynamics: Inferences from Laurentide eskers, Canada. *Geomorphology*, *32*(3–4), 263–293. https://doi.org/10.1016/S0169-555X(99)00100-2

Chandler, B. M. P., Lovell, H., Boston, C. M., Lukas, S., Barr, I. D., Benediktsson, ÍÖ, Benn, D. I., Clark, C. D., Darvill, C. M., Evans, D. J. A., Ewertowski, M. W., Loibl, D., Margold, M., Otto, J. C., Roberts, D. H., Stokes, C. R., Storrar, R. D., & Stroeven, A. P. (2018). Glacial geomorphological mapping: A review of approaches and frameworks for best practice. *Earth-Science Reviews*, *185*, 806–846. https://doi.org/10.1016/j.earscirev.2018.07.015

Clague, J. J., & Ward, B. (2011). Pleistocene glaciation of British Columbia. *Developments in Quaternary Science*, *15*, 563–573. https://doi.org/10.1016/B978-0-444-53447-7.00044-1

Clark, C. D. (1999). Glaciodynamic context of subglacial bedform generation and preservation. *Annals of Glaciology*, *28*, 23–32. https://doi.org/10.3189/172756499781821832

Clark, C. D., Ely, J. C., Greenwood, S. L., Hughes, A. L. C., Meehan, R., Barr, I. D., Bateman, M. D., Bradwell, T., Doole, J., Evans, D. J. A., Jordan, C. J., Monteys, X., Pellicer, X. M., & Sheehy, M. (2018). BRITICE Glacial Map, version 2: A map and GIS database of glacial landforms of the last British-Irish Ice sheet. *Boreas*, *47*(1), 11–e8. https://doi.org/10.1111/bor.12273

Dalton, A. S., Margold, M., Stokes, C. R., Tarasov, L., Dyke, A. S., Adams, R. S., Allard, S., Arends, H. E., Atkinson, N., Attig, J. W., Barnett, P. J., Barnett, R. L., Batterson, M., Bernatchez, P., Borns, H. W., Breckenridge, A., Briner, J. P., Brouard, E., Campbell, J. E., … Wright, H. T. (2020). An updated radiocarbon-based ice margin chronology for the last deglaciation of the North American Ice Sheet complex. *Quaternary Science Reviews*, *234*, 106223. https://doi.org/10.1016/j.quascirev.2020.106223

Davis, N. F. G., & Mathews, W. H. (1944). Four phases of glaciation with illustrations from southwestern British Columbia. *The Journal of Geology*, *52*(6), 403–413. https://doi.org/10.1086/625236

Dunlop, P., & Clark, C. D. (2006). The morphological characteristics of ribbed moraine. *Quaternary Science Reviews*, *25*(13-14), 1668–1691. https://doi.org/10.1016/j.quascirev.2006.01.002

Dyke, A. S. (2004). An outline of North American deglaciation with emphasis on central and northern Canada. In J. Ehlers & P. I. Gibbard (Eds.), *Quaternary glaciations – extent and chronology, part II* (pp. 373–424). Elsevier. https://doi.org/10.1016/S1571-0866(04)80209-4

Dyke, A. S., Moore, A., & Robertson, L. (2003). Deglaciation of North America: Thirty two digital maps at 1:7,000,000 scale with accompanying digital chronological database and one poster (two sheets) with full maps series. Geological Survey of Canada Open File 1574. https://doi.org/10.4095/214399

Dyke, A. S., & Prest, V. K. (1987). *Paleogeography of northern North America, 18 000–5 000 years ago. Map 1703A*. Geological Survey of Canada. https://doi.org/10.4095/133927

Evans, D. (2005). Ice-marginal terrestrial landsystems: Active temperate glacier margins. In D. Evans (Ed.), *Glacial landsystems* (pp. 12–43). Hodder.

Fulton, R. J. (1991). A conceptual model for growth and decay of the Cordilleran Ice sheet. *Géographie Physique et Quaternaire*, *45*(3), 281–286. https://doi.org/10.7202/032875ar

Gabrielse, H. (1963). *McDame map area, Cassiar distruct, British Columbia*. British Columbia. Geological Survey of Canada, Memoir 319. https://doi.org/10.4095/100546

Gabrielse, H. (1988). *Geology of Cry Lake and Dease Lake map areas, north-central British Columbia*. Geological Survey of Canada, Bulletin 504. https://doi.org/10.4095/210074

German Aerospace Center. (2018). *TanDEM-X – Digital Elevation Model (DEM) – Global, 12 m*. https://gdk.gdi-de.org/geonetwork/srv/api/records/5eecdf4c-de57-4624-99e9-60086b032aea. Accessed January 15, 2020.

Government of Canada. (2019). Canadian Digital Elevation Model, 1945–2011. Available at https://open.canada.ca/data/en/dataset/7f245e4d-76c2-4caa-951a-45d1d2051333. Accessed November 1, 2018.

Greenwood, S. L., & Clark, C. D. (2009). Reconstructing the last Irish Ice Sheet 1: Changing flow geometries and ice flow dynamics deciphered from the glacial landform record. *Quaternary Science Reviews*, *28*(27–28), 3085–3100. https://doi.org/10.1016/j.quascirev.2009.09.008

Greenwood, S. L., Clark, C. D., & Hughes, A. L. C. (2007). Formalising an inversion methodology for reconstructing ice-sheet retreat patterns from meltwater channels: Application to the British Ice sheet. *Journal of Quaternary Science*, *22*(6), 637–645. https://doi.org/10.1002/jqs.1083

Greenwood, S. L., Clason, C. C., Helanow, C., & Margold, M. (2016). Theoretical, contemporary observational and palaeo-perspectives on ice sheet hydrology: Processes and products. *Earth-Science Reviews*, *155*, 1–27. https://doi.org/10.1016/j.earscirev.2016.01.010

Hättestrand, C., & Kleman, J. (1999). Ribbed moraine formation. *Quaternary Science Reviews*, *18*(1), 43–61. https://doi.org/10.1016/S0277-3791(97)00094-2

Hebrand, M., & Åmark, M. (1989). Esker formation and glacier dynamics in eastern skane and adjacent areas, southern Sweden. *Boreas*, *18*(1), 67–81. https://doi.org/10.1111/j.1502-3885.1989.tb00372.x

Hewitt, I. J., & Creyts, T. T. (2019). A model for the formation of eskers. *Geophysical Research Letters*, *46*(12), 6673–6680. https://doi.org/10.1029/2019GL082304

Jansson, K. N., Kleman, J., & Marchant, D. R. (2002). The succession of ice-flow patterns in north-central Québec-Labrador, Canada. *Quaternary Science Reviews*, *21*(4–6), 503–523. https://doi.org/10.1016/S0277-3791(01)00013-0

King, E. C., Hindmarsh, R. C. A., & Stokes, C. R. (2009). Formation of mega-scale glacial lineations observed beneath a west Antarctic ice stream. *Nature Geoscience*, *2*(8), 585–588. https://doi.org/10.1038/ngeo581

Klassen, R. W. (1978). *Surficial geology of Rancheria River, Swift River, Tagish, Takhini River, southern Yukon*. Geological Survey of Canada, open file 539, 1:100,000 scale. https://doi.org/10.4095/129393

Kleman, J., Hättestrand, C., Borgström, I., & Stroeven, A. (1997). Fennoscandian palaeoglaciology reconstructed using a glacial geological inversion model. *Journal of Glaciology*, *43*(144), 283–299. https://doi.org/10.1017/S0022143000003233

Kleman, J., Jansson, K., De Angelis, H., Stroeven, A. P., Hättestrand, C., Alm, G., & Glasser, N. (2010). North American Ice Sheet build-up during the last glacial cycle, 115–21 kyr. *Quaternary Science Reviews*, *29*(17–18), 2036–2051. https://doi.org/10.1016/j.quascirev.2010.04.021

Lakeman, T. R., Clague, J. J., & Menounos, B. (2008). Advance of alpine glaciers during final retreat of the Cordilleran ice sheet in the Finlay river area, northern British Columbia, Canada. *Quaternary Research*, *69*(2), 188–200. https://doi.org/10.1016/j.yqres.2008.01.002

Livingstone, S. J., Storrar, R. D., Hillier, J. K., Stokes, C. R., Clark, C. D., & Tarasov, L. (2015). An ice-sheet scale comparison of eskers with modelled subglacial drainage routes. *Geomorphology*, *246*, 104–112. https://doi.org/10.1016/j.geomorph.2015.06.016

Lundqvist, J. (1989). Rogen (ribbed) moraine – identification and possible origin. *Sedimentary Geology*, *62*(2–4), 281–292. https://doi.org/10.1016/0037-0738(89)90119-X

Mannerfelt, J. M. (1949). Marginal drainage channels as indicators of the gradients of Quaternary ice caps. *Geografiska Annaler*, *31*, 194–199.

Margold, M., & Jansson, K. N. (2012). Evaluation of data sources for mapping glacial meltwater features. *International Journal of Remote Sensing*, *33*(8), 2355–2377. https://doi.org/10.1080/01431161.2011.608738

Margold, M., Jansson, K. N., Kleman, J., & Stroeven, A. P. (2011). Glacial meltwater landforms of central British Columbia. *Journal of Maps*, *7*(1), 486–506. https://doi.org/10.4113/jom.2011.1205

Margold, M., Jansson, K. N., Kleman, J., & Stroeven, A. P. (2013a). Lateglacial ice dynamics of the Cordilleran Ice Sheet in northern British Columbia and southern Yukon Territory: Retreat pattern of the Liard Lobe reconstructed from the glacial landform record. *Journal of Quaternary Science*, *28*(2), 180–188. https://doi.org/10.1002/jqs.2604

Margold, M., Jansson, K. N., Kleman, J., Stroeven, A. P., & Clague, J. J. (2013b). Retreat pattern of the Cordilleran Ice Sheet in central British Columbia at the end of the last glaciation reconstructed from glacial meltwater landforms. *Boreas*, *42*, n/a–n/a. https://doi.org/10.1111/bor.12007

Margold, M., Stokes, C. R., & Clark, C. D. (2018). Reconciling records of ice streaming and ice margin retreat to produce a palaeogeographic reconstruction of the deglaciation of the Laurentide Ice Sheet. *Quaternary Science Reviews*, *189*, 1–30. https://doi.org/10.1016/j.quascirev.2018.03.013

Margold, M., Stroeven, A. P., Clague, J. J., & Heyman, J. (2014). Timing of terminal Pleistocene deglaciation at high elevations in southern and central British Columbia constrained by ^{10}Be exposure dating. *Quaternary Science Reviews*, *99*, 193–202. https://doi.org/10.1016/j.quascirev.2014.06.027

Mathews, W. H. (1986). *Physiographic map of the Canadian Cordillera*. Geological Survey of Canada, A series map 1701A, sheet 1. https://doi.org/10.4095/122821

Mathews, W. H., Gabrielse, H., & Rutter, N. W. (1975). *Glacial maps of Beatton river map area, British Columbia. Geological Survey of Canada, open file 274, 1:1,000,000 scale*. https://doi.org/10.4095/129373

Menounos, B., Goehring, B. M., Osborn, G., Margold, M., Ward, B., Bond, J., Clarke, G. K. C., Clague, J. J., Lakeman, T., Koch, J., Caffee, M. W., Gosse, J., Stroeven, A. P., Seguinot, J., & Heyman, J. (2017). Cordilleran Ice Sheet mass loss preceded climate reversals near the Pleistocene termination. *Science*, *358*(6364), 781–784. https://doi.org/10.1126/science.aan3001

Norris, S. L., Margold, M., & Froese, D. G. (2017). Glacial landforms of northwest Saskatchewan. *Journal of Maps*, *13*(2), 600–607. https://doi.org/10.1080/17445647.2017.1342212

Planet Team. (2017). *Planet application program interface: In space for life on earth*. https://api.planet.com

Plouffe, A. (1996). *Surficial geology, Tsayta Lake, British Columbia (93N/SW)*. Geological Survey of Canada, open file 3071, 1:000,000 scale. https://doi.org/10.4095/207500

Plouffe, A. (1997). *Surficial geology, Manson Creek, British Columbia (93N/NE)*. Geological Survey of Canada, open file 3312, 1:000,000 scale. https://doi.org/10.4095/208661

Plouffe, A. (2000). *Surficial geology, Manson River, British Columbia*. Geological Survey of Canada, Map 1987A, 1:250,000 scale. https://doi.org/10.4095/211398

Prest, V. K., Grant, D. R., & Rampton, V. N. (1968). *Glacial map of Canada, Map scale 1:5,000,000*. Geological Survey of Canada, Map 1467A. https://doi.org/10.4095/108979

Ryder, J. M., & Maynard, D. (1991). The cordilleran ice sheet in Northern British Colombia. *Géographie Physique et Quaternaire*, *45*(3), 355–363. https://doi.org/10.7202/032881ar

Shaw, J., Sharpe, D., & Harris, J. (2010). A flowline map of glaciated Canada based on remote sensing data. *Canadian Journal of Earth Sciences*, *47*(1), 89–101. https://doi.org/10.1139/E09-068

Shreve, R. L. (1985). Esker characteristics in terms of glacier physics, Katahdin esker system, Maine. *Geological Society of America Bulletin*, *96*(5), 639–646. https://doi.org/10.1130/0016-7606(1985)96<639:ECITOG>2.0.CO;2

Stokes, C. R., Margold, M., & Creyts, T. (2016). Ribbed bedforms on palaeo-ice stream beds resemble regular patterns of basal shear stress ('traction ribs') inferred from modern ice streams. *Journal of Glaciology*, *62*(234), 696–713. https://doi.org/10.1017/jog.2016.63

Stokes, C. R., Tarasov, L., Blomdin, R., Cronin, T. M., Fisher, T. G., Gyllencreutz, R., Hättestrand, C., Heyman, J., Hindmarsh, R. C. A., Hughes, A. L. C., Jakobsson, M., Kirchner, N., Livingstone, S. J., Margold, M., Murton, J. B., Noormets, R., Peltier, W. R., Peteet,

D. M., Piper, D. J. W., … Teller, J. T. (2015). On the reconstruction of palaeo-ice sheets: Recent advances and future challenges. *Quaternary Science Reviews*, *125*, 15–49. https://doi.org/10.1016/j.quascirev.2015.07.016

Storrar, R. D., Ewertowski, M., Tomczyk, A. M., Barr, I. D., Livingstone, S. J., Ruffell, A., Stoker, B. J., & Evans, D. J. A. (2020). Equifinality and preservation potential of complex eskers. *Boreas*, *49*(1), 211–231. https://doi.org/10.1111/bor.12414

Storrar, R. D., Stokes, C. R., & Evans, D. J. A. (2014). Morphometry and pattern of a large sample (>20,000) of Canadian eskers and implications for subglacial drainage beneath ice sheets. *Quaternary Science Reviews*, *105*, 1–25. https://doi.org/10.1016/j.quascirev.2014.09.013

Stroeven, A. P., Hättestrand, C., Kleman, J., Heyman, J., Febel, D., Fredin, O., Goodfellow, B. W., Harbor, J. M., Jansen, J. D., Olsen, L., Caffee, M. W., Fink, D., Lundqvist, J., Rosqvist, G. C., Strömberg, B., & Jansson, K. N. (2016). Deglaciation of Fennoscandia. *Quaternary Science Reviews*, *147*, 91–121. https://doi.org/10.1016/j.quascirev.2015.09.016

Stumpf, A. J., Broster, B. E., & Levson, V. M. (2000). Multiphase flow of the late Wisconsinan Cordilleran ice sheet in western Canada. *Geological Society of America Bulletin*, *112*(12), 1850–1863. https://doi.org/10.1130/0016-7606(2000)1121850:MFOTLW>2.0.CO;2

Turner, A. J., Woodward, J., Stokes, C. R., Ó Cofaigh, C, & Dunning, S. (2014). Glacial geomorphology of the great glen region of Scotland. *Journal of Maps*, *10*(1), 159–178. https://doi.org/10.1080/17445647.2013.866369